AD-A083 919 NAVAL RESEARCH LAB WASHINGTON DC F/G 20/3
ELECTROMAGNETIC SCATTERING PATTERNS FROM SINUSOIDAL SURFACES: V--ETC(U)
MAR 80 R H LANG, A K JORDAN
UNCLASSIFIED NRL-MR-4188 NL

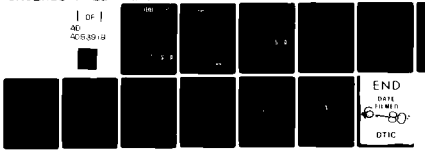

LEVEL II

(12)

NRL Memorandum Report 4188

Electromagnetic Scattering Patterns from Sinusoidal Surfaces: Vertical Polarization

R. H. LANG AND A. K. JORDAN

Aerospace Systems Branch
Space Systems Division

March 17, 1980

NAVAL RESEARCH LABORATORY
Washington, D.C.

UNCLASSIFIED

SECURITY CLASSIFICATION OF THIS PAGE (When Data Entered)

REPORT DOCUMENTATION PAGE	READ INSTRUCTIONS BEFORE COMPLETING FORM
1. REPORT NUMBER: NRL Memorandum Report 4188 — 2. GOVT ACCESSION NO.: AD-A083 919	3. RECIPIENT'S CATALOG NUMBER:
4. TITLE (and Subtitle): ELECTROMAGNETIC SCATTERING PATTERNS FROM SINUSOIDAL SURFACES: VERTICAL POLARIZATION	5. TYPE OF REPORT & PERIOD COVERED: Interim report on a continuing NRL problem
	6. PERFORMING ORG. REPORT NUMBER:
7. AUTHOR(s): R. H. Lang and A. K. Jordan	8. CONTRACT OR GRANT NUMBER(s): ONR 79-0732-0-0
9. PERFORMING ORGANIZATION NAME AND ADDRESS: Naval Research Laboratory, Washington, DC 20375	10. PROGRAM ELEMENT, PROJECT, TASK AREA & WORK UNIT NUMBERS: 61153N-31; RR021-01-41; 79-0732-0-0
11. CONTROLLING OFFICE NAME AND ADDRESS	12. REPORT DATE: March 17, 1980
	13. NUMBER OF PAGES: 17
14. MONITORING AGENCY NAME & ADDRESS(if different from Controlling Office)	15. SECURITY CLASS. (of this report): UNCLASSIFIED
	15a. DECLASSIFICATION/DOWNGRADING SCHEDULE

16. DISTRIBUTION STATEMENT (of this Report)

Approved for public release; distribution unlimited

17. DISTRIBUTION STATEMENT (of the abstract entered in Block 20, if different from Report)

18. SUPPLEMENTARY NOTES

19. KEY WORDS (Continue on reverse side if necessary and identify by block number)

Scattering patterns	Periodic surfaces
Sinusoidal surfaces	Rough surfaces
Vertical polarization	Electromagnetic scattering

20. ABSTRACT (Continue on reverse side if necessary and identify by block number)

In this paper we present an analysis and calculation of scattering patterns resulting from a vertically polarized beam of electromagnetic plane waves incident on a sinusoidal surface. This model is frequently used to study scattering from periodically rough surfaces. The horizontally-polarized case is treated in a previous paper by the authors. The vector properties of this electromagnetic scattering problem are considered in this communication by extending the previous analysis to the vertically-polarized case and comparing the scattering patterns for the two polarizations.

DD FORM 1 JAN 73 1473 EDITION OF 1 NOV 68 IS OBSOLETE
S/N 0102-014-6601

UNCLASSIFIED

SECURITY CLASSIFICATION OF THIS PAGE (When Data Entered)

CONTENTS

ELECTROMAGNETIC SCATTERING PATTERNS FROM SINUSOIDAL SURFACES: VERTICAL POLARIZATION

INTRODUCTION

In this paper we present an analysis and calculation of scattering patterns resulting from a vertically polarized beam of electromagnetic plane waves incident on a sinusoidal surface. This model is frequently used to study scattering from periodically rough surfaces. The horizontally-polarized case is treated in a previous paper [1] by the authors which contains more detailed discussion and references. The vector properties of this electromagnetic scattering problem are considered in this communication by extending the previous analysis to the vertically-polarized case and comparing the scattering patterns for the two polarizations.

Electromagnetic waves that are scattered from periodically rough surfaces have a characteristic dependence on the observation angle. In addition to scattering at the specular angle, which is characteristic of reflection from a smooth plane, these waves also scatter at a discrete number of different angles, due to the rough nonplanar nature of the surface.

The fields scattered from periodically rough surfaces can be computed by employing the space-harmonic representation. This representation expresses the scattered field as a discrete sum of space harmonics (plane waves). The scattering coefficient associated with each space harmonic is calculated after the application of an exact boundary condition on the surface. The polarization of the incident electromagnetic wave relative to the sinusoidal surface determines the type of boundary condition (Dirichlet or Neumann) that is used.

Note: Manuscript submitted January 15, 1980.

The previous analysis of the scattering patterns [1] has been generalized to include both vertically and horizontally polarized electromagnetic waves. The scattering of acoustic (scalar) waves from a sinusoidal surface has been analyzed by DeSanto [2]. Whitman and Schwering [3] have independently obtained a similar formulation for the electromagnetic surface currents for both the horizontal and vertical cases and have compared their calculations with the direct numerical solutions of the integral equations for the surface currents.

REPRESENTATION OF THE ELECTROMAGNETIC FIELDS

The electromagnetic field scattered from a sinusoidal surface is represented by a superposition of plane waves which consists of a discrete spectrum of space harmonics. In general, the electromagnetic field incident on the surface can be analyzed in terms of two orthogonally polarized components: horizontal and vertical. In the horizontal case (denoted by a superscript (H)) the total $\underline{E}$ field is parallel to the y axis; $\underline{E} = \underline{a_y}\,\psi^{(H)}(x,z)$ where $\underline{a_y}$ is a unit vector in the y direction. In the vertical case (denoted by a superscript (V)) the total $\underline{H}$ field is parallel to the y axis; $\underline{H} = \underline{a_y}\psi^{(V)}(x,z)$. The total field amplitude above the z = 0 plane is composed of the incident and scattered field amplitudes

$$\psi^{(q)}(x,z) = \psi_o(x,z) + \psi_{sc}^{(q)}(x,z), \quad q \in \{H,V\}. \tag{1}$$

The spatial dependence of the incident plane wave is

$$\psi_o(x,z) = e^{ik(\alpha_o x - \beta_o z)}, \quad z \geq 0 \tag{2}$$

where $k = 2\pi/\lambda$ is the wavenumber and $\alpha_o = \sin\theta_i$ and $\beta_o = \cos\theta_i$. Here θ_i is the angle of incidence measured with respect to the z axis. The

space-harmonic representation of the scattered field is

$$\psi_{sc}^{(q)}(x,z) = \sum_{n=-\infty}^{\infty} R_n^{(q)} e^{ik(\alpha_n x + \beta_n z)}, \quad z \geq 0 \tag{3}$$

where $R_n^{(q)}$ is the scattering coefficient of the nth space harmonic, $\alpha_n = \sin\theta_n$, $\beta_n = \cos\theta_n$, and θ_n is the scattering angle of the nth space harmonic as shown in Figure 1. We note that the angle of specular reflection is θ_o and $\theta_o = \theta_i$.

The profile, s(x), of the surface shown in Figure 1 is a sinusoid with period ℓ and amplitude d

$$s(x) = -\frac{d}{2}\left(1 + \cos\frac{2\pi}{\ell} x\right). \tag{4}$$

Due to the periodicity of the surface, the normalized transverse wavenumbers, α_n, satisfy the grating equation.

$$\alpha_n = \alpha_o + n\Lambda, \quad n = \pm 1, \pm 2, \ldots, \tag{5}$$

where $\Lambda = \lambda/\ell$, and

$$\beta_n = \sqrt{1 - \alpha_n^2}, \quad \mathrm{Im}(\beta_n) \geq 0. \tag{6}$$

The scattering coefficient, $R_n^{(q)}$ can be calculated by applying Green's second theorem to the region bounded by the curve C, as is shown in Figure 1. We have

$$\int_C \left[\psi^{(q)} \frac{\partial G^{\pm}}{\partial n} - G^{\pm} \frac{\partial \psi}{\partial n}^{(q)}\right] d\mu = 0, \tag{7}$$

where

$$G^{\pm} = e^{ik(\pm\beta_n z - \alpha_n x)} \tag{8}$$

Here μ is the arc length along the contour C and $\underline{n}$ is the inward normal. Along that portion of the contour on the sinusoidal surface, the boundary condition is used to simplify the integral in (7). The vanishing of the tangential $\underline{E}$ field on the surface of the conductor implies that $\psi^{(H)} = 0$ (Dirichlet condition) and $\frac{\partial \psi}{\partial n}^{(V)} = 0$ (Neumann condition) on the surface.

By using the above boundary conditions in the integral equation (7) expressions for the scattering coefficients $R_n^{(q)}$ are obtained ([3] and [2])

$$R_m^{(q)} = e^{i\tau_m^+} \sum_{n=-\infty}^{\infty} V_{mn}^{(q)} a_n^{(q)} \quad , \; m = 0, \pm 1, \pm 2, \ldots \tag{9}$$

where

$$V_{mn}^{(H)} = - i^m \frac{\beta_m}{\beta_o} J_{m-n}(\tau_m^+), \tag{10}$$

$$V_{mn}^{(V)} = i^m (1+b_{mn}) J_{m-n}(\tau_m^+) \tag{11}$$

$$b_{mn} = \frac{\alpha_m(\alpha_m - \alpha_n)}{\beta_m(\beta_m + \beta_o)} \tag{12}$$

Here J_n is the nth-order Bessel function with argument

$$\tau_m^{\pm} = \Delta(\beta_o \pm \beta_m), \; \Delta = \pi d/\lambda. \tag{13}$$

The $a_n^{(q)}$ that appear in (9) are the coefficients of the Fourier expansion of the surface currents and thus will be called the surface current amplitudes. They satisfy the following infinite system of equations:

$$\sum_{n=-\infty}^{\infty} T_{mn}^{(q)} a_n^{(q)} = \delta_{m,o} \quad , \; m = 0, \pm 1, \ldots \tag{14}$$

where

$$T_{mn}^{(H)} = J_{m-n}(\tau_m^-) \tag{15}$$

$$T_{mn}^{(V)} = \begin{cases} (1 - \beta_o\beta_m - \alpha_m\alpha_n) J_{m-n}(\tau_m^-), & m = \pm 1, \pm 2, \ldots \\ \delta_{n,o} + c\delta_{n,1} + c\delta_{n,-1}, & m = 0 \end{cases} \tag{16}$$

with $c = i\Delta\Lambda\alpha_o/(2\beta_o)$ and $\delta_{m,n}$ is the Kronecker delta function:

$$\delta_{m,n} = \begin{cases} 1, & m = n \\ 0, & m \neq n \end{cases}$$

CALCULATION OF SCATTERING COEFFICIENTS - VERTICAL POLARIZATION

The infinite set of linear equations (14) can be solved numerically for the $\left\{a_n^{(q)}\right\}$ by symmetrically truncating the system at an order M and solving the resulting 2M-order matrix equation. More accuracy is obtained by sequentially increasing M; this technique is known as the method of reduction.

Confidence in this numerical method for solving the set of equations (14) was established by employing two criteria: conservation of energy and solution stability. For a lossless surface the conservation of energy criterion requires that the incident power be equal to the scattered power. Employing Poynting's theorem, we have (z^* is the complex conjugate of z)

$$k\beta_o \ell = \int_{-\ell/2}^{+\ell/2} \mathrm{Re}\left(i\psi_{sc}^{(q)} \frac{\partial \psi_{sc}^{(q)^*}}{\partial z}\right) dx. \tag{17}$$

If we introduce the normalized reflection coefficients

$$|\Gamma_n^{(q)}|^2 = |R_n^{(q)}|^2 \frac{\beta_n}{\beta_o}, \tag{18}$$

and use (3) in (17), then energy conservation requires that

$$1 = \sum_{n \in P} |\Gamma_n^{(q)}|^2, \tag{19}$$

where the sum is only over the set of propagating modes P, $P = \{n:\mathrm{Im}(\beta_n)=0\}$. The conservation criterion can now be written as

$$\lim_{M \to \infty} \varepsilon_M = 0, \tag{20}$$

where

$$\varepsilon_M = \left|1 - \sum_{n \in P} |\Gamma_n(M)|^2\right|. \tag{21}$$

Here ε_M is the energy-conservation error made when the approximate reflection coefficient, $\Gamma_n(M)$, is used; the $\Gamma_n(M)$ are obtained when the $\{a_n\}$ have been computed after truncating system (14) to order M.

The other criterion used was a check of the stability of the matrix solutions. The complex values of a symmetric subset of the surface current amplitudes $\{a_n\}$ should stabilize with increasing matrix size 2M for a given

set of parameters θ_i, Λ, Δ. In all cases which we examined, the energy-conservation and current-stabilization criteria were compatible.

The above numerical procedure was carried out for five different sets of parameters in both the horizontally and vertically polarized cases. The results are shown in Table I. The first two examples use the same surface parameters that were used in [1], Example 1. In these cases both the perturbation and physical-optics conditions, as defined in [1], are exceeded. The last three examples show Bragg backscattering. Examples three and four demonstrate first-order Bragg backscattering, while example five shows second-order Bragg backscattering. The energy-conservation criterion was applied with the following steps: First, M was chosen large enough to include the set P of all propagating modes; second, M was incremented until $\varepsilon_M \leq 10^{-4}$, if this criterion hadn't been satisfied during the calculations for the first step. In Table I the values of normalized height, Δ, and period, Λ, of the surface are given along with the angle of incidence, θ_i. We also shown the maximum matrix order needed to establish an accuracy ε_M.

Because of the interest in radar backscatter, we have used our numerical procedure to calculate the absolute value of the Bragg backscattering amplitude $|\Gamma_{-1}|$. The plots are shown in Figure 2 as a function of the normalized roughness amplitude for several different values of Bragg backscattering angle $\theta_{B,-1} = \arcsin(\Lambda/2)$. For small values of Δ, the backscattering amplitude depends linearly on Δ; however, the slope of this line approaches zero as $\theta_{B,-1} \to \pi/2$ (grazing). This indicates that a perturbation theory could be used for small $\theta_{B,-1}$ but it would have limited validity as $\theta_{B,-1} \to \pi/2$. As Δ increases the curves oscillate between 0 and 1. The maximum value that each curve attains is 1 as can be seen from (19). We also note that when $|\Gamma_{-1}| = 1$, all other Γ_n, $n \neq -1$, are zero because of energy conservation.

Thus, at this maximum all incident energy is backscattered to the transmitter; this phenomenon is known as blazing. It is interesting to observe that all curves shown in Figure 2 that attain the value 1 on the first oscillation have only two propagating modes. Thus the curves for $\theta_{B,-1} = 75^{\circ}$ and 85° do not reach 1 on its first oscillation and have more than two modes propagating. We also note that the curves have been terminated at different values of Δ; this is due to limitations of the computer program whose convergence is parameter dependent.

CALCULATION OF SCATTERING PATTERNS

The scattering pattern $S^{(q)}(\theta)$ is defined as

$$S^{(q)}(\theta) = \lim_{r\to\infty} \frac{kr}{4\pi} |\psi_{sc}^{(q)}|^2 . \tag{22}$$

The scattered intensity, $\psi_{sc}^{(q)}$, can be calculated as a function of observation angle when a bounded beam is incident on the surface. Let us assume that the incident beam is given as

$$\psi_o^{(q)}(x,z) = W\left[(x+z\tan\theta_i)/L\right] e^{ik(\alpha_o x - \beta_o z)}, \tag{23}$$

where the beam is centered about the line $x = -z \tan\theta_i$. The beam shape is defined by the function $W(x/L)$ which is slowly varying when $|x| \leq L/2$ and $W(x/L) = 0$ for $|x| > L/2$. If we decompose the incident beam into plane waves, a space harmonic representation can be obtained for the scattered field $\psi_{sc}^{(q)}$.

An exact expression for the scattering pattern in the horizontally-polarized case is derived in [1] by using the space harmonic representation of the scattered field in (22). Since the arguments used there hold equally well in the vertically-polarized case, we have

$$S^{(q)}(\theta) = \left|\sum_{n\in P}^{Q} \left[kL(\sin\theta - \sin\theta_n)\right] R_n^{(q)}(\sin\theta - n\Lambda)\right|^2, \tag{24}$$

where

$$Q(kL\sigma) = \frac{kL}{2\pi} \int_{-\infty}^{\infty} W(\bar{x}) e^{ikL\sigma\bar{x}} d\bar{x} \ . \qquad (25)$$

Here Q can be interpreted as the scattering amplitude due to an incident beam on the z = 0 plane. In addition, we note that only propagating space harmonics contribute to $S^{(q)}(\theta)$.

To use (24), one requires the knowledge of $R_n^{(q)}$ at many different angles of incidence. When kL is large, an approximate expression can be obtained which only requires $R_n^{(q)}$ at the angle of incidence of the beam. Following the arguments of [1], we have

$$S^{(q)}(\theta) = \left| \sum_{n \in P} Q(kL(\sin\theta - \sin\theta_n)) \cdot R_n^{(q)}(\sin\theta_i) \right|^2 \qquad (26)$$

The validity of (26) is based on the fact that $R_n^{(q)}(\sin\theta_i)$ must be a slowly varying function of θ_i compared to the variation of the Q function.

DISCUSSION

The exact formula (26) for the horizontally- or vertically-polarized scattering patterns will differ only in the scattering coefficients $R_n^{(H)}$ or $R_n^{(V)}$. Thus the behavior of $R_n^{(H)}$ and $R_n^{(V)}$ as functions of the input parameters θ_i, Λ, and Δ (we recall that Λ and Δ contain the incident electromagnetic wavelength λ) will reveal the behavior of the corresponding scattering patterns. For example, the graphs of $R_n^{(H)}$ and $R_n^{(V)}$ as functions of incidence angle, which we call the space-harmonic diagrams, have been extensively studied for periodic surfaces (see, for example, [3], Figs. 3 and 4). These diagrams reveal the existence and relative strengths of the various propagating space harmonics. The graphs of $R_n^{(H)}$ and $R_n^{(V)}$ as functions of Δ reveal the existence of blazing; the existence of Bragg backscatter blazing is shown in Fig. 2.

We first repeated all the numerical examples of Table 1 in [1] for the case of vertical polarization. Since some of these examples did not differ significantly between the two polarizations, we varied the input parameters (θ_i, Λ, Δ) to demonstrate several interesting effects of polarization and these are summarized in Table 1. However, in the interests of brevity, only scattering patterns for the case of blazing (Example 4 and Figs. 3 and 4) will be shown here.

Example 1, provides a straightforward demonstration of the scattering pattern calculation. However, for this example the vertically and horizontally-polarized cases happen to be similar at $\theta_i = 45^o$, which was discussed in [1], Example 1. An examination of the space harmonic plots reveals that changing the incidence angle to 30^o, as in example 2, provides a clearer distinction between the scattering patterns for the horizontally- and vertically-polarized cases.

The third and fourth examples demonstrate first-order Bragg backscattering. The vertically-polarized scattering pattern for example 3 is not significantly different from the corresponding horizontally-polarized case ([1], Fig. 7) for $\theta_i = 45^o$. However, if the incidence angle is adjusted to the blazing angle, $\theta_i = 60^o$, as in example 4, there is substantial difference between the horizontally-polarized (Fig. 3) and vertically-polarized (Fig. 4) cases. Finally, example 5 demonstrates the case of vertically-polarized second-order Bragg backscatter; comparison with the horizontally-polarized case of [1], Fig. 8, shows that the specular and backscatter components are larger for this vertical-polarization case.

REFERENCES

1. A. K. Jordan and R. H. Lang, "Electromagnetic Scattering Patterns from Sinusoidal Surfaces", Radio Science, 14, p. 1077-1088, 1979.

2. J. A. DeSanto, "Scattering from a Sinusoid: Derivation of Linear Equations for the Field Amplitudes", J. Acoustic Soc. Am. 57, p. 1195-1197, 1975.

3. G. Whitman, and F. Schwering, "Scattering by Periodic Metal Surfaces with Sinusoidal Height Profiles -- a Theoretical Approach", IEEE Trans. Antennas and Propag., AP-25, p. 869-876, 1977.

ACKNOWLEDGEMENT

The authors gratefully acknowledge the competent Fortran programming and computer calculations of Mrs. D. Duncan.

TABLE 1. Parameters for scattering pattern calculations.

Example	Polarization	Λ	Δ	$\sigma_m = \Delta\Lambda$, max. slope	θ_i	No. of Propagating Modes	Max. Matrix Order 2M	Energy Conservation Error ε_M
1	Vert. / Hor.	.40	2.356	0.942	45	5	20 / 28	1.45×10^{-5} / 8.58×10^{-8}
2	Vert. / Hor.	.40	2.356	0.942	30	5	26 / 22	1.38×10^{-5} / 5.03×10^{-5}
3	Vert. / Hor.	$\sqrt{2}$	1.50	2.121	45	2	20 / 22	2.71×10^{-5} / 1.10×10^{-6}
4	Vert. / Hor.	1.73	.60	1.038	60	2	10 / 10	1.04×10^{-5} / 3.03×10^{-6}
5	Vert. / Hor.	$\sqrt{2}/2$	1.11	0.785	45	3	14 / 18	5.45×10^{-6} / 2.17×10^{-8}

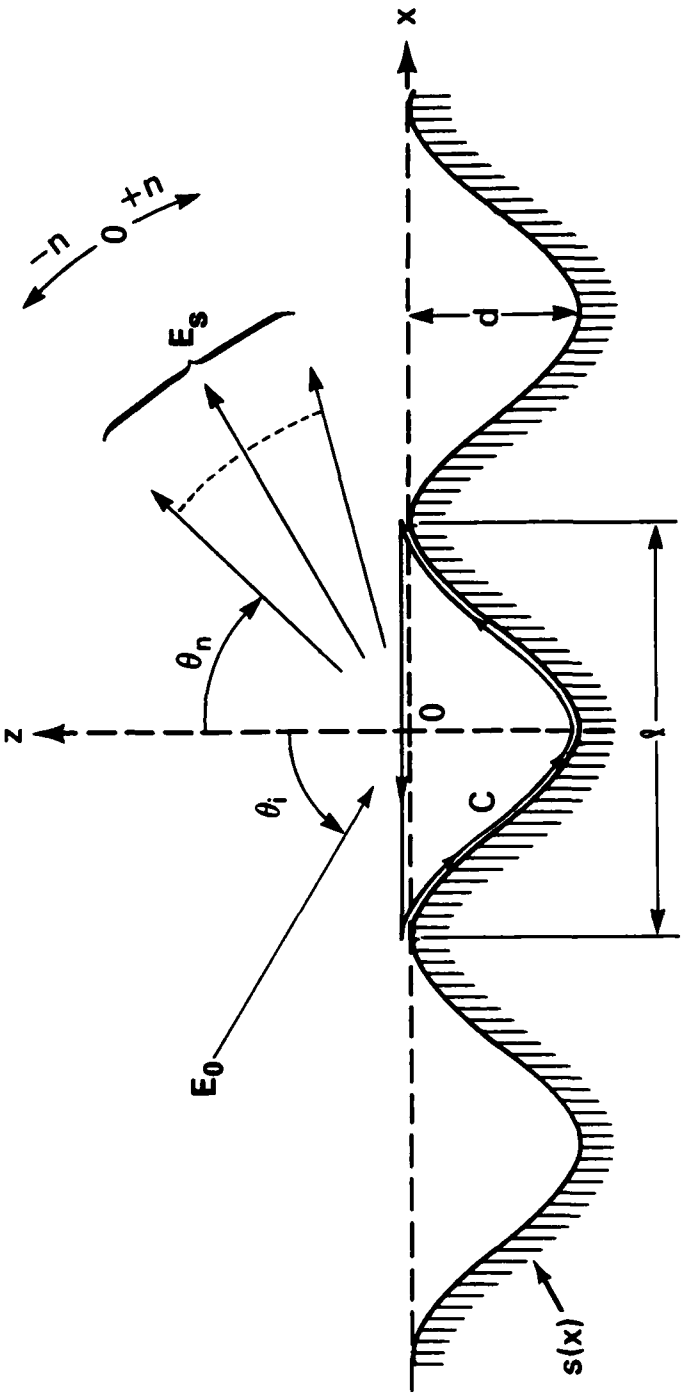

Fig. 1. Plane wave scattering by a sinusoidal surface, s(x).

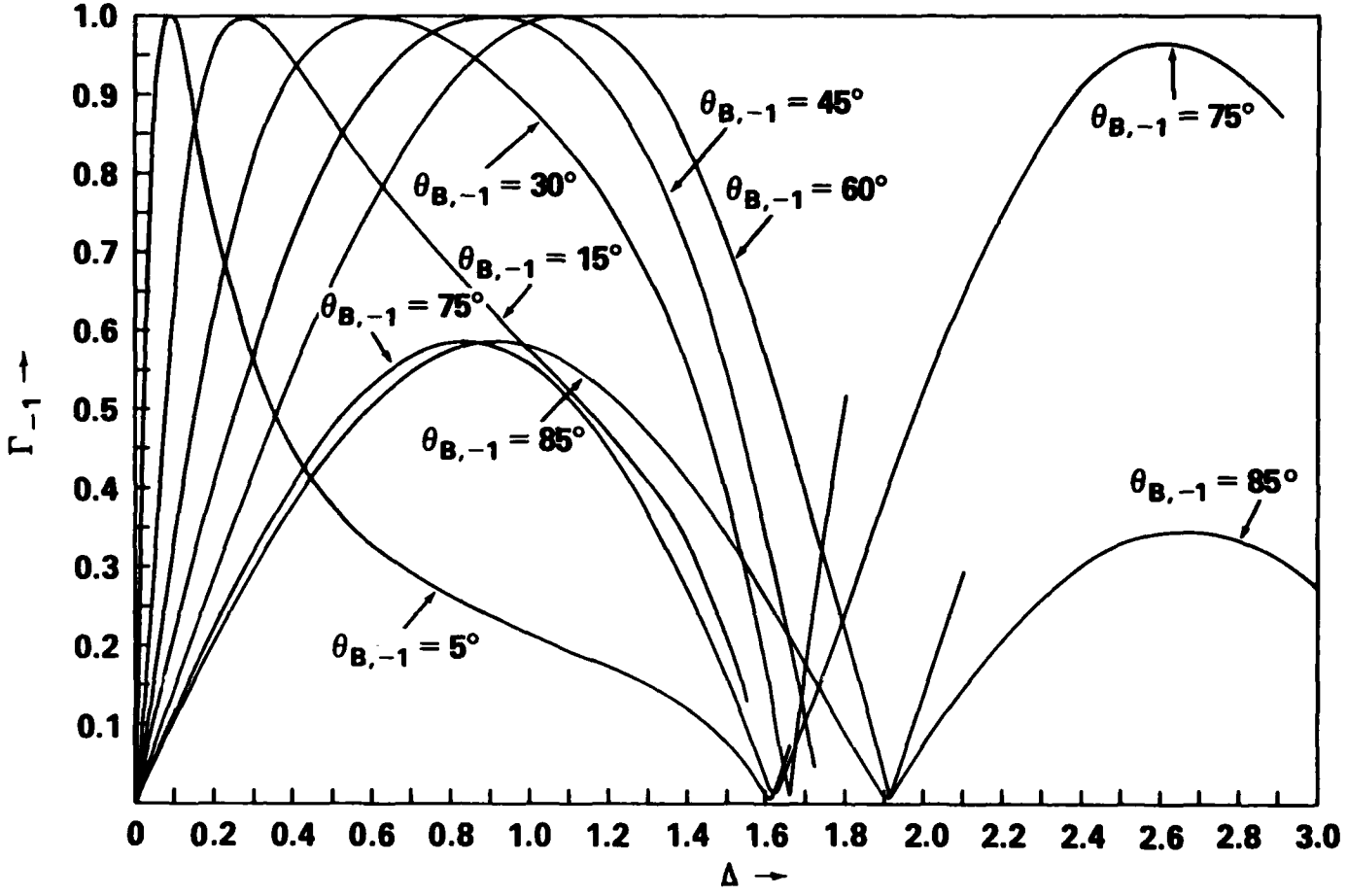

Fig. 2. Bragg backscattering amplitude, $|\Gamma_{-1}^{(V)}|$, vs. roughness parameter, Δ, for vertical polarization.

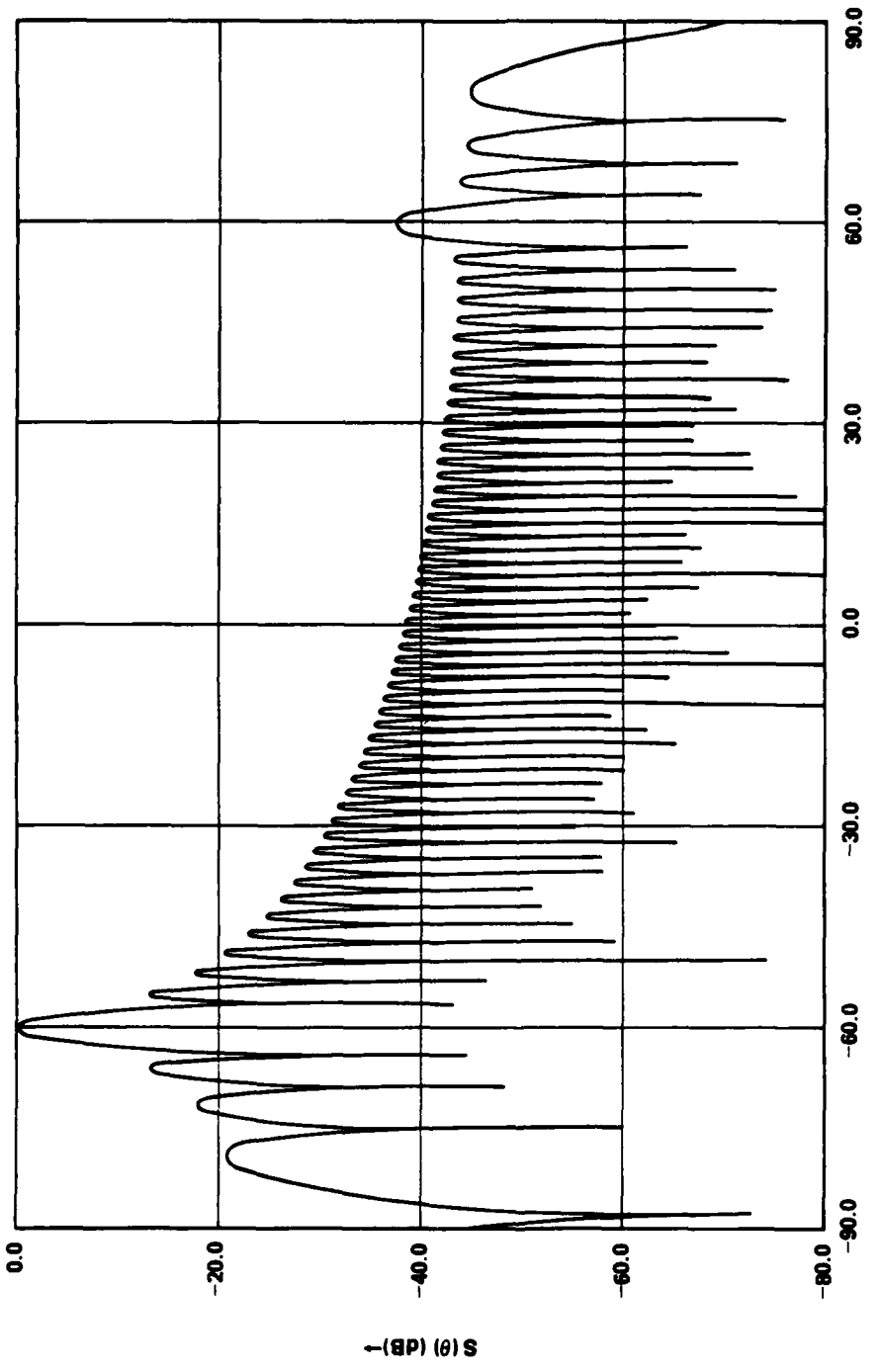

Fig. 3. Scattering pattern, $S(\theta)$, vs. scattering angle, θ, for example 4 (vertical polarization).

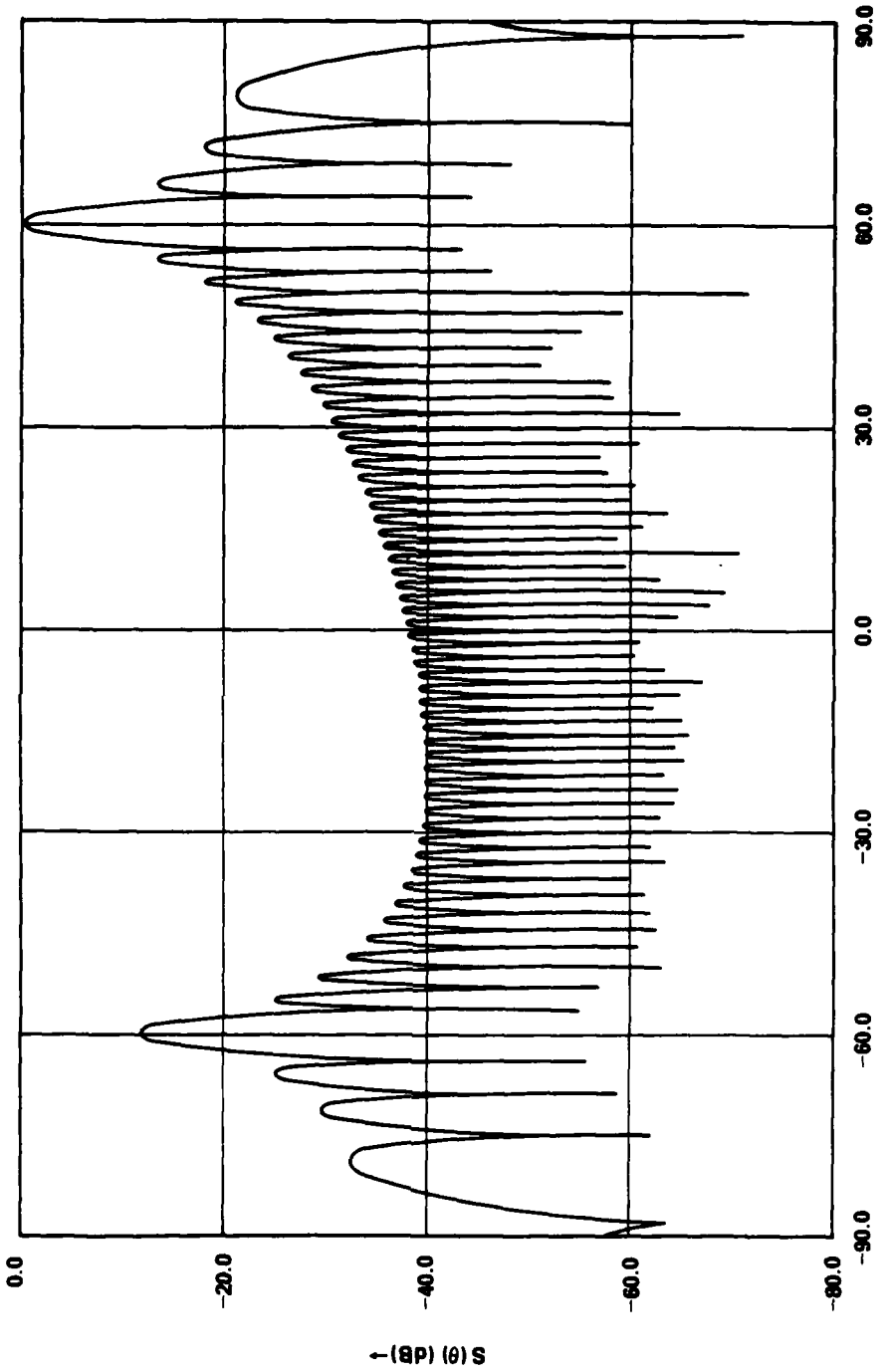

Fig. 4. Scattering pattern for example 4 (horizontal polarization).